

Origin of the soft p_T spectra

G. Gatoff and Cheuk-Yin Wong

Center for Computationally Intensive Physics and Physics Division, Oak Ridge National Laboratory, Oak Ridge, Tennessee 37831-6373

(Received 6 March 1992)

In high-energy collisions, the soft p_T spectra for produced mesons contain information on the motion of the quarks and antiquarks which form these mesons. We extract this information in the context of the flux-tube model with Schwinger's mechanism for particle production. We solve the Dirac equation for quarks (and antiquarks) inside a flux tube, described as an infinitely long cylinder of radius r_0 , with a uniform electric field κ inside it. We calculate the production rate of quarks, antiquarks, and pions as a function of p_T . We study first a sharp transverse boundary, and find that the result deviates from the experimental soft p_T spectra, with its characteristic exponential fall. We therefore introduce a scalar potential which varies smoothly in the radial direction. With simplifying assumptions we show how the experimental p_T spectra of pions, created in p - p collisions, determine the transverse wave function and the scalar potential that would produce it. The classical turning point for this potential is of the order of 0.6 fm. However, the potential flattens out considerably beyond that point. The wave function decays as $r^{-3/2}$ and there appears to be a considerable excursion of the quark into regions far beyond the classical turning point.

PACS number(s): 13.85.Ni, 12.40.Aa, 25.75.+r

I. INTRODUCTION

In the process of particle production, the origin of the transverse momentum distribution for soft particles ($p_T \lesssim 2.5$ GeV/ c) remains one of the unsolved puzzles. In the simple model of the Schwinger mechanism [1,2], one often assumes capacitor plates which have an infinite extension in the transverse directions [3,4]. The produced quarks and antiquarks have a transverse momentum p_T and hence a transverse mass $m_T = \sqrt{m_0^2 + p_T^2}$, where m_0 is the rest mass of the quark. Thus, the transverse momentum acts as a mass which has to tunnel through a barrier in the longitudinal direction to lead to the production of $q\bar{q}$ pairs [1,3]. The produced q 's will later combine with \bar{q} 's to form the observed mesons. The tunneling of the transverse mass gives rise to a probability distribution for the transverse momentum of the quarks in the form

$$\exp[-\pi(p_T^2 + m_0^2)/\kappa]. \quad (1.1)$$

Although the root-mean-squared value of the transverse momentum of the observed pions (~ 0.37 GeV/ c) is approximately consistent with a simple estimate from Eq. (1.1) [$(\sqrt{2\kappa/\pi}) \sim 0.35$ GeV/ c] with a string tension of $\kappa = 1$ GeV/fm, there are many conceptual problems with such an explanation. First, the observed distribution [5,6] is better described in terms of an exponential function $\exp(-p_T/T)$ or $\exp(-m_T/T)$. This differs from the Gaussian shape (1.1) expected from infinite parallel plates. Second, the concept of confinement suggests a color electric flux in a limited region in the transverse direction, so the treatment of two parallel plates of infinite extension is not appropriate. The effects of a transverse boundary have been studied by Martin and Vautherin [7]. Using the Schwinger proper time method

and the Balian-Bloch multiple reflection expansion of Green's functions, they calculated the pair production in a unified electric field confined in a limited volume in space. Their result, however, is for the overall production rate, excluding the detailed momentum profile.

The transverse momentum distribution of the produced particles has well been reviewed [6]. In several papers, the confining radial potential is taken to be that of the MIT bag model, or an equivalent boundary condition. Pavel and Brink [8] have solved the Dirac equation by separating it into longitudinal and transverse components. Although they introduced a spatially dependent mass term, it was applied to a square well with a sharp boundary. In their work, and also in the work of Schönfeld *et al.* [9] and Sailer *et al.* [10], they had a boundary condition that gave a particle distribution of oscillating Bessel functions of the transverse momentum. The absence of such oscillations in experimental data [5,6] raises the question of whether a bag model description for the transverse direction is realistic or not.

It is clear from the outset that the p_T spectra of soft particles reveal the motion of the produced particles in the transverse degrees of freedom. This distribution can be used to provide information on the motion of the constituents of the mesons. Let us assume that the observed mesons, such as pions, come from the combination of a quark and an antiquark. If so, the distribution of the observed pion comes from the convolution of the momentum of the quark with that of the antiquark. In this paper, we show that the $q\bar{q}$ pairs are produced mainly in their ground state of their transverse degrees of freedom. Assuming they stay in that state, the p_T spectra of pions provide direct information on the transverse momentum distribution of q and \bar{q} . From this information, we can infer the shape of the effective potential that the quark and the antiquark experience during the process of their

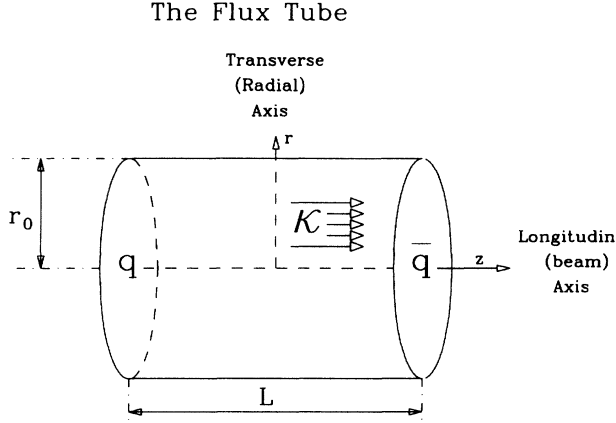


FIG. 1. Schematic picture of the flux tube, as a cylinder of length L and radius r_0 . Inside there is a uniform field κ . Outside the field is zero.

production.

We carry out such a program with the soft p_T spectra for nucleon-nucleon collisions and find the shape of the effective potential for the quark and antiquark. Not surprisingly, the potential one extracts rise sharply in the region inside the "flux tube." The classical turning point for the quark is of the order of 0.6 fm. The motion to the region beyond the classical turning point is, however, considerable, as the effective potential flattens out at large values of transverse distances, and the height of the potential above the effective energy of the quark is not large. In the radial cylindrical coordinate r , the wave function goes like $r^{-3/2}$ for large r .

In our model the flux-tube is described as a cylinder of length L and of radius r_0 , with a uniform electric field κ inside it and zero everywhere outside (see Fig. 1). In the next section we define the problem, and apply the separation of the Dirac equation into longitudinal and transverse components, as shown by Pavel and Brink [8]. The longitudinal equation is the same equation as for the one-dimensional problem of two infinite capacitor plates, previously solved by Wang and Wong [4]. In this paper, we are interested in the transverse direction only. In Sec. III we study the radial equation with a square well potential, given by a small mass inside the tube and an infinite mass outside it. Such a potential leads to a boundary condition equivalent to the one given by the MIT bag model. We show that this result does not agree with the experimental p_T spectra. In Sec. IV we allow the scalar potential to vary smoothly with the radial coordinate $m = m(r)$. We show how the soft p_T spectra can be used to obtain the ground-state wave function and the transverse characteristics of the potential. In Sec. V we summarize and present our conclusions.

II. SEPARATING THE DIRAC EQUATION TO LONGITUDINAL AND TRANSVERSE DIRECTIONS

In applying the Schwinger particle production mechanism to nucleon-nucleon collisions, we envisage that after

the projectile hits the target a quark from one nucleon combines with a diquark from the other to form a flux tube. Two such tubes will be formed in each nucleon-nucleon collision. The leading quark-diquark pairs act like $q\bar{q}$ strings and provide an external color field between them where new $q\bar{q}$ pairs can be produced [3]. We shall assume that the field created by the leading quark and antiquark (or diquark) can be approximated by an Abelian gauge field A_μ . Quarks and antiquarks are spontaneously produced in this field when a quark tunnels from the negative energy continuum to the positive one. The interaction potential is gA_μ , where g is the charge which is positive for a quark and negative for an antiquark. We wish to confine both quarks and antiquarks with the same transverse effective potential (with the same sign). It is therefore proper to introduce an external *scalar* potential [8] $m(r)$ which contains the rest mass of the quark and does not distinguish between quarks and antiquarks. The Dirac equation for the quark is

$$[\gamma^\mu(p_\mu - gA_\mu) - m]\psi = 0. \quad (2.1)$$

Let us choose the gauge so that $\mathbf{A} = 0$ and $A_0 = A_0(z)$. In that case Eq. (2.1) becomes

$$[\boldsymbol{\alpha} \cdot \mathbf{p} + gA_0(z) + \beta m(r)]\psi = E\psi. \quad (2.2)$$

Separation of variables is possible if one assumes the form

$$\begin{pmatrix} \psi_1 \\ \psi_2 \\ \psi_3 \\ \psi_4 \end{pmatrix} = \begin{pmatrix} \rho_1(r, \phi)\varphi_1(E, z) \\ -\rho_2(r, \phi)\varphi_2(E, z) \\ \rho_1(r, \phi)\varphi_2(E, z) \\ \rho_2(r, \phi)\varphi_1(E, z) \end{pmatrix}. \quad (2.3)$$

Inserting these into the Dirac equation, one can introduce the separation constant m^* , so that the equation decouple to the form [8]

$$\begin{pmatrix} -(m^* - m) & p_- \\ p_+ & -(m^* + m) \end{pmatrix} \begin{pmatrix} \rho_1(r, \phi) \\ \rho_2(r, \phi) \end{pmatrix} = 0, \quad (2.4)$$

where $p_\pm = p_x \pm ip_y$, and

$$\begin{pmatrix} (gA_0 - E + m^*) & p_z \\ p_z & (gA_0 - E - m^*) \end{pmatrix} \begin{pmatrix} \varphi_1(E, z) \\ \varphi_2(E, z) \end{pmatrix} = 0. \quad (2.5)$$

For the longitudinal part, let us write

$$\begin{aligned} \varphi_1 &= \sigma_1(E, z) + \sigma_2(E, z), \\ \varphi_2 &= \sigma_1(E, z) - \sigma_2(E, z). \end{aligned} \quad (2.6)$$

In this case, Eq. (2.5) becomes

$$\begin{pmatrix} [gA_0(z) - E] + p_z & m^* \\ m^* & [gA_0(z) - E] - p_z \end{pmatrix} \begin{pmatrix} \sigma_1(E, z) \\ \sigma_2(E, z) \end{pmatrix} = 0. \quad (2.7a,b)$$

Inserting (2.7a) into (2.7b) and vice versa one obtains

$$[\{gA_0(z)-E\}^2 + ig\partial_z A_0(z) + \partial_z^2 - m^{*2}] \sigma_1 = 0. \quad (2.8)$$

The equation for σ_2 is just the complex conjugate of (2.8). Therefore, if one solution corresponds to an incoming

$$gA_0(z) = \begin{cases} 0 & \text{for } z \leq -L/2 \text{ (region I),} \\ -\kappa(z+L/2) & \text{for } -L/2 \leq z \leq L/2 \text{ (region II),} \\ -\kappa L & \text{for } L/2 \leq z \text{ (region III).} \end{cases} \quad (2.9)$$

In the regions where A_0 is constant (I and III), the solution of (2.8) is

$$\sigma_1(z) = \exp(ik_z z), \quad \sigma_2(z) = \exp(-ik_z z), \quad (2.10)$$

with the dispersion relation

$$(gA_0 - E)^2 = m^{*2} + k_z^2, \quad (2.11)$$

where A_0 is different for region I and region III. In region II the solution is a hypergeometric function given by Wang and Wong [4]. Knowing the wave function, it is possible to calculate the rate of pair production. This was also calculated [4] and shown to be equivalent to the pair production rate obtained first by Schwinger [1]. The transmission rate for $L \rightarrow \infty$ is

$$|T|^2 \propto \exp\left[-\frac{\pi m^{*2}}{\kappa}\right], \quad (2.12)$$

and the pair production rate is

$$\frac{dN}{d^4x} = -\frac{2N_c}{4\pi^2} \kappa \int_0^\infty dp_T p_T \ln(1 - e^{-\pi(m^{*2})/\kappa}), \quad (2.13)$$

where $2N_c$ is the degeneracy, as we have $(2s+1)N_c$ for spin $s = \frac{1}{2}$ particles of color degeneracy N_c . Schwinger's calculation has been repeated and generalized for time-dependent fields by Brezin and Itzykson [2] and by Herrmann and Knoll [11]. It was shown to be useful for particle production in QCD by Casher *et al.* [3].

Let us now turn to the radial equation. The explicit form of (2.4) is

$$\begin{aligned} p_- \rho_2(r, \phi) + [m(r) - m^*] \rho_1(r, \phi) &= 0, \\ p_+ \rho_1(r, \phi) - [m(r) + m^*] \rho_2(r, \phi) &= 0, \end{aligned} \quad (2.14)$$

where

$$p_+ \equiv -i \left[\frac{\partial}{\partial x} + i \frac{\partial}{\partial y} \right] = -ie^{i\phi} \left[\frac{\partial}{\partial r} + \frac{i}{r} \frac{\partial}{\partial \phi} \right], \quad (2.15)$$

$$p_- \equiv -i \left[\frac{\partial}{\partial x} - i \frac{\partial}{\partial y} \right] = -ie^{-i\phi} \left[\frac{\partial}{\partial r} - \frac{i}{r} \frac{\partial}{\partial \phi} \right].$$

The angular and radial dependence can be further separated with the assertion

wave, the other solution corresponds to an outgoing wave. Equation (2.8) is identical to the one-dimensional problem for infinitely parallel plates solved by Wang and Wong [4], replacing m_T with m^* , and choosing the vector potential

$$\rho_1 = R_{1\nu}(r) e^{i\nu\phi}, \quad \rho_2 = iR_{2\nu}(r) e^{i(\nu+1)\phi}, \quad \nu = 0, \pm 1, \pm 2, \dots \quad (2.16)$$

This gives the coupled equations

$$\left[\frac{\partial}{\partial r} + \frac{\nu+1}{r} \right] R_{2\nu}(r) + [m(r) - m^*] R_{1\nu}(r) = 0, \quad (2.17a)$$

$$\left[\frac{\partial}{\partial r} - \frac{\nu}{r} \right] R_{1\nu}(r) + [m(r) + m^*] R_{2\nu}(r) = 0. \quad (2.17b)$$

Equation (2.17) is the radial equation to be solved for a given scalar potential $m(r)$.

III. SQUARE WELL BOUNDARY CONDITIONS

This is the case solved by Pavel and Brink [8] and also by Schönfeld *et al.* [9] and Sailer *et al.* [10]. In this case, the boundary condition is $m(r) = m_0$ for $r < r_0$, where m_0 is the current quark mass, and $m(r) = M \rightarrow \infty$ for $r > r_0$. Solving Eqs. (2.17a) and (2.17b) on the boundary [8] for $r = r_0 + \epsilon$ and $r = r_0 - \epsilon$ gives the condition

$$R_{1\nu}(r_0) = R_{2\nu}(r_0). \quad (3.1)$$

One can solve Eq. (2.17) with $m(r) = m_0$ for $r < r_0$. The solution is

$$R_{1\nu}(r) = A_1 J_\nu(Cr), \quad R_{2\nu}(r) = A_2 J_{\nu+1}(Cr), \quad (3.2)$$

where J_ν are the Bessel functions of the first kind of order ν . Equation (3.2) solves (2.17) with the dispersion relation [8]

$$m^{*2} = C^2 + m_0^2 \implies m_\pm^* = \pm \sqrt{C^2 + m_0^2}, \quad (3.3)$$

and

$$\left[\frac{A_2}{A_1} \right]_\pm = \pm \frac{C_\pm}{\sqrt{C_\pm^2 + m_0^2} \pm m_0} = \pm \frac{\sqrt{C_\pm^2 + m_0^2} \mp m_0}{C_\pm}. \quad (3.4)$$

Defining $x_\pm \equiv C_\pm r_0$, the boundary condition (3.1) with the assertion (3.2) and (3.3) and (3.4) implies

$$J_{\nu\pm 1}(x_\pm) = \pm f(x_\pm) J_\nu(x_\pm), \quad (3.5)$$

where

$$f(x) = \frac{\sqrt{x^2 + (m_0 r_0)^2} \pm m_0 r_0}{x}.$$

Here we have a discrete set of allowed values for $C_{\nu,s,\pm}$ where $\nu=0,1,2,\dots$ correspond to the azimuthal quantum number, and the s correspond to the s th solutions of (3.5) for each ν . The \pm correspond to the two solutions

$$\psi_{\nu+1/2,s,\pm}(E_{\nu,s,\pm}, C_{\nu,s,\pm}) = \begin{pmatrix} A_1(C_{\nu,s,\pm})J_\nu(C_{\nu,s,\pm}r)e^{i\nu\phi} \\ -iA_2(C_{\nu,s,\pm})J_{\nu+1}(C_{\nu,s,\pm}r)e^{i(\nu+1)\phi} \\ A_1(C_{\nu,s,\pm})J_\nu(C_{\nu,s,\pm}r)e^{i\nu\phi} \\ iA_2(C_{\nu,s,\pm})J_{\nu+1}(C_{\nu,s,\pm}r)e^{i(\nu+1)\phi} \end{pmatrix} \sigma_1(C_{\nu,s,\pm}, E_{\nu,s,\pm}, z). \quad (3.6)$$

(The $\nu+1/2$ is just a label associated with the angular momentum of that function [8].) This result becomes interesting only after performing a Fourier transform onto momentum space. This was realized by Schönfeld *et al.* [9] and Sailer *et al.* [10]. Let us define

$$\mathcal{J}_{\nu,s,\pm}(p_T r) = \frac{1}{2\pi} \int_0^{r_0} dr r \int_0^{2\pi} d\phi e^{-ip_T r \sin\phi} J_\nu(C_{\nu,s,\pm}r) e^{i\nu\phi}. \quad (3.7)$$

Equation (3.7) becomes

$$\begin{aligned} \mathcal{J}_{\nu,s,\pm}(p_T r_0) &= \int_0^{r_0} dr r J_\nu(p_T r) J_\nu(C_{\nu,s,\pm}r) \\ &= \frac{r_0}{p_T^2 - C_{\nu,s,\pm}^2} [-C_{\nu,s,\pm} J_\nu(p_T r_0) J_{\nu+1}(C_{\nu,s,\pm}r_0) + p_T J_{\nu+1}(p_T r_0) J_\nu(C_{\nu,s,\pm}r_0)]. \end{aligned} \quad (3.8)$$

This result was obtained by Schönfeld *et al.* [9] and Sailer *et al.* [10], and also the transformed wave function

$$\psi_{\nu+1/2,s,\pm}(E_{\nu,s,\pm}, C_{\nu,s,\pm}) = \begin{pmatrix} A_1(C_{\nu,s,\pm})\mathcal{J}_{\nu,s,\pm}(p_T r_0) \\ -iA_2(C_{\nu,s,\pm})\mathcal{J}_{\nu+1,s,\pm}(p_T r_0) \\ A_1(C_{\nu,s,\pm})\mathcal{J}_{\nu,s,\pm}(p_T r_0) \\ iA_2(C_{\nu,s,\pm})\mathcal{J}_{\nu+1,s,\pm}(p_T r_0) \end{pmatrix} \sigma_1(C_{\nu,s,\pm}, E_{\nu,s,\pm}, z). \quad (3.9)$$

These wave functions have to be normalized, but we shall ignore the normalization for the time being. The current j_z becomes

$$\begin{aligned} j_z &= \bar{\psi} \gamma_z \psi = \psi^\dagger \begin{pmatrix} 0 & \sigma_z \\ \sigma_z & 0 \end{pmatrix} \psi \\ &= 2 \left[|A_1 \mathcal{J}_{\nu,s,\pm}(p_T r_0)|^2 + |A_2 \mathcal{J}_{\nu+1,s,\pm}(p_T r_0)|^2 \right] |\sigma_1(E_{\nu,s,\pm}, z)|^2. \end{aligned} \quad (3.10)$$

When $z \rightarrow \infty$, the factor $|\sigma_1|^2$ is just the transmission probability $|T|^2$ for a normalized wave coming from $z \rightarrow -\infty$. For an infinitely long cylinder ($L \rightarrow \infty$) it will have the form (2.12). We remind the reader that the c number m^{*2} in (2.12) is each one of the eigenvalues of the coupled radial equations (2.17a) and (2.17b). Once derived, they will each be substituted in the longitudinal equation (2.8), which is itself an eigenvalue equation for the eigenvalues E . The probability of producing a q and a \bar{q} is proportional to the current [4]

$$\mathcal{P}_{\nu,s,\pm} \propto |j_z(z \rightarrow +\infty)|. \quad (3.11)$$

Comparing to the case of two parallel plates with infinite transverse extension [4], the current is now multiplied by a new factor which previously was equal to 1. Therefore,

$$\mathcal{P}_{\nu,s,\pm} \rightarrow |T|^2 \left[|A_1 \mathcal{J}_{\nu,s,\pm}|^2 + |A_2 \mathcal{J}_{\nu+1,s,\pm}|^2 \right] \times \text{normalization}. \quad (3.12)$$

The ratio between A_1 and A_2 is given by (3.3)–(3.5). The probability of creating a pair out of the vacuum (in the area $\Delta x \Delta y$) will be given by

$$\mathcal{P}_{v,s,\pm} = -\ln \left[1 - \exp \left\{ -\frac{\pi(C_{v,s,\pm}^2 + m^2)}{\kappa} \right\} \right] \frac{1}{\Delta x \Delta y} \\ \times \mathcal{N}_{v,s,\pm}^{-1} \left\{ |J_{v+1}(C_{v,s,\pm} r_0)|^2 |\mathcal{J}_{v,s,\pm}(p_0 r_0)|^2 + |J_v(C_{v,s,\pm} r_0)|^2 |\mathcal{J}_{v+1,s,\pm}(p_T r_0)|^2 \right\}. \quad (3.13)$$

The total number of pairs produced out of the vacuum will be

$$dN_q = \text{phase space} \times \text{probability} = 2N_c dx dy dz \frac{dp_x}{2\pi} \frac{dp_y}{2\pi} \frac{dp_z}{2\pi} \sum_{v,s,\pm} \mathcal{P}_{v,s,\pm}. \quad (3.14)$$

However $dz = v_z dt = p_z dt/E \Rightarrow dp_z dz = dp_z(p_z/E)dt = dE dt$. For a constant field κ , $dE = \kappa dz$ and $dp_x dp_y = 2\pi dp_T p_T$ and, therefore,

$$\frac{dN_q}{dt dz p_T dp_T} = 2N_c \frac{\kappa}{4\pi^2} \sum_{v,s,\pm} \mathcal{P}_{v,s,\pm} = -2N_c \frac{\kappa}{4\pi^2} \sum_{v,s,\pm} \ln \left[1 - \exp \left\{ -\frac{\pi(C_{v,s,\pm}^2 + m^2)}{\kappa} \right\} \right] \\ \times \mathcal{N}_{v,s,\pm}^{-1} \left\{ |J_{v+1}(C_{v,s,\pm} r_0)|^2 |\mathcal{J}_{v,s,\pm}(p_T r_0)|^2 + |J_v(C_{v,s,\pm} r_0)|^2 |\mathcal{J}_{v+1,s,\pm}(p_T r_0)|^2 \right\}, \quad (3.15a)$$

where

$$\mathcal{N}_{v,s,\pm} = \int_0^\infty 2\pi dp_T p_T \left\{ |J_{v+1}(C_{v,s,\pm} r_0)|^2 |\mathcal{J}_{v,s,\pm}(p_T r_0)|^2 + |J_v(C_{v,s,\pm} r_0)|^2 |\mathcal{J}_{v+1,s,\pm}(p_T r_0)|^2 \right\}. \quad (3.15b)$$

In Appendix A we show that in the limit where $r_0 \rightarrow \infty$, we recover the Schwinger expression. This was not shown by Pavel and Brink [8], nor by Schönfeld *et al.* [9] who derived the limit only for the total rate integrated over all momentum space. The result (3.15) is presented in Fig. 2 with $\kappa = 1$ GeV/fm. A different value of κ would change the overall cross section, but not the shape of the p_T spectra. This is due to the exponential weight in (3.15), which will make the state with the lowest energy dominant over all others. The high p_T dependence falls off like p_T^{-3} , as seen from (3.15) and (3.8). The oscillations in Fig. 2 are characteristic of Bessel functions. Note that Eq. (3.15) and Fig. 2 are for the creation rate of pairs of quarks and antiquarks, and not of pions. Nevertheless, combining the momenta of a quark and an antiquark to form a pion (see next section), we will not be able to produce the typical $\exp(-p_T/T)$ falloff. The low p_T has a Gaussian shape, and the high p_T has oscillations. This indicates that the square well is unrealistic as a quantitative description of the transverse motion of the produced quarks.

IV. THE SCALAR POTENTIAL

The soft p_T spectra of the mesons contain information on the transverse motion of the quarks and antiquarks which form them. In the preceding section, we learned that the p_T distribution of those quarks is related to their radial wave function inside the flux tube. Knowing the wave function, we can find out the potential that pro-

duces it. There is no *a priori* reason to justify an effective potential with a sharp boundary. We therefore introduce a smoothly varying scalar potential $m^2(r)$. Changing the potential will result in a change of the wave function and the p_T spectra. By inserting (2.17b) into (2.17a) and vice versa, we obtain the equations

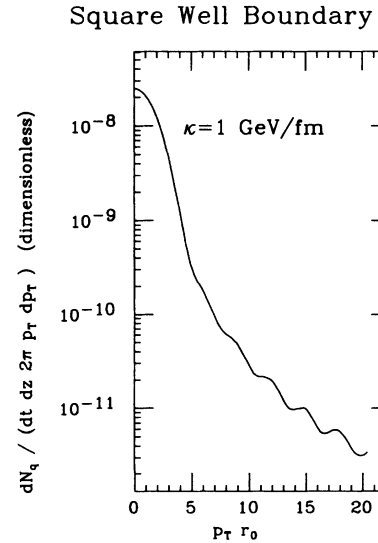


FIG. 2. The rate of creating q 's and \bar{q} 's with a sharp boundary at $r = r_0$. A different value of κ will not change the general shape (see text). The wiggles result from the Bessel function J_0 .

$$\begin{aligned} \frac{\partial^2}{\partial r^2} R_{1\nu}(r) + \frac{1}{r} \frac{\partial}{\partial r} R_{1\nu}(r) - \frac{\nu^2}{r^2} R_{1\nu}(r) \\ + [m^{*2} - m^2(r)] R_{1\nu}(r) = -R_{2\nu}(r) \frac{\partial}{\partial r} m(r) \\ \frac{\partial^2}{\partial r^2} R_{2\nu}(r) + \frac{1}{r} \frac{\partial}{\partial r} R_{2\nu}(r) - \frac{(\nu+1)^2}{r^2} R_{2\nu}(r) \\ + [m^{*2} - m^2(r)] R_{2\nu}(r) = -R_{1\nu}(r) \frac{\partial}{\partial r} m(r). \end{aligned} \quad (4.1)$$

Equations (4.1) are like two Schrödinger equations with an effective potential of the form $m^2(r)$ and “energy eigenvalues” equal to m^{*2} . This is not entirely correct since the equations are coupled, but if one neglects the $m'(r)$ on the right-hand sides, the equations decouple. A scalar potential is a reasonable effective potential because it acts on both the quarks and antiquarks in the same manner. In fact, the electric field κ should not be uniform along the radial axis, and it should vary smoothly unless there is “perfect confinement.” Furthermore, incorporating the gluons with all the components of the Yang-Mills fields is also missing here. We therefore allow ourselves to include a space-dependent mass, which to some extent may account for effects that were left out.

Let us now introduce a general scalar potential $m(r)$ and follow the same procedure as in the previous section. Substituting (2.16) into the wave function (2.3), and also (2.6) with σ_1 only, the wave function is given by

$$\psi_{\nu+1/2,s,\pm}(E_{\nu,s,\pm}) = \begin{pmatrix} R_{1\nu}(r)e^{i\nu\phi} \\ -iR_{2\nu}(r)e^{i(\nu+1)\phi} \\ R_{1\nu}(r)e^{i\nu\phi} \\ iR_{2\nu}(r)e^{i(\nu+1)\phi} \end{pmatrix} \sigma_1(E_{\nu,s,\pm}, z). \quad (4.2)$$

$$\frac{dN_q}{dt dz p_T dp_T} = -2N_c \frac{\kappa}{4\pi^2} \sum_{\nu,s,\pm} \ln \left[1 - \exp \left[-\frac{\pi m_{\nu,s,\pm}^{*2}}{\kappa} \right] \right] \left[|\mathcal{R}_{1\nu,s,\pm}(p_T)|^2 + |\mathcal{R}_{2\nu,s,\pm}(p_T)|^2 \right], \quad (4.5)$$

where $\mathcal{R}(\mathbf{p}_T) = \mathcal{R}(p_T)$ is the (two-dimensional) Fourier transform of $R(r)e^{i\nu\phi}$. Note that from now on we shall use script characters such as $\mathcal{R}(p_T)$ for Fourier transforms to momentum space of functions $R(r)e^{i\nu\phi}$ in configuration space carrying the same capital italic letter. We do not know what $m(r)$ should be in (4.1). On the other hand, we know the pion p_T spectra from experiment. Assuming that a pion is a combination of quark and an antiquark, we can obtain the p_T spectra for the quarks. For simplicity, we neglect the time evolution, the hadronization, and several other effects. Since (4.5) contains the Fourier transform $\mathcal{R}_\nu(p_T)$, one can Fourier transform backwards to find $R_\nu(r)e^{i\nu\phi}$, and find the scalar potential $m(r)$ which will fit the data [5]. This is generally not possible, since (4.5) contains a sum. It will only be possible if there is a dominant term, as there is in the case of a square well. In that case

$$\frac{dN_q}{dt dz p_T dp_T} \propto \mathcal{P}_q(p_T) \propto |\mathcal{R}(p_T r_0)|^2, \quad (4.6)$$

This is a generalization of Eq. (3.6). Just as in the previous section, ν is the azimuthal quantum number s , corresponds to the number of nodes, and \pm to be positive and negative values of m^* . After a Fourier transform the wave function will be

$$\psi_{\nu+1/2,s,\pm}(E_{\nu,s,\pm}) = \begin{pmatrix} \mathcal{R}_{1\nu}(p_T)e^{i\nu\phi} \\ -i\mathcal{R}_{2\nu}(p_T)e^{i(\nu+1)\phi} \\ \mathcal{R}_{1\nu}(p_T)e^{i\nu\phi} \\ i\mathcal{R}_{2\nu}(p_T)e^{i(\nu+1)\phi} \end{pmatrix} \sigma_1(E_{\nu,s,\pm}, z). \quad (4.3)$$

This more general relation replaces Eq. (3.9). The current j_z given by (3.10) for the square well is now given by

$$\begin{aligned} j_z = \bar{\psi} \gamma_z \psi = \psi^\dagger \begin{pmatrix} 0 & \sigma_z \\ \sigma_z & 0 \end{pmatrix} \psi \\ = 2 \left[|\mathcal{R}_{1\nu,s,\pm}(p_T)|^2 + |\mathcal{R}_{2\nu,s,\pm}(p_T)|^2 \right] |\sigma_1(E_{\nu,s,\pm}, z)|^2 \end{aligned} \quad (4.4)$$

Suppose we solve (4.1) and find all the solutions for $R_{1\nu}(r)$, $R_{2\nu}(r)$, and m^* . Comparing (4.4) and (3.10), and examining (2.12), (2.13) and (3.3), the production rate for the quarks (and antiquarks) (3.15) becomes

where $\mathcal{R} \equiv \mathcal{R}_{1,\nu=0,s=0,+}$ and $\mathcal{P}_q(p_T)$ is the probability for creating a quark with transverse momentum p_T , which is equal to the probability for creating an antiquark with equal transverse momentum $\mathcal{P}_{\bar{q}}(p_T)$. The state $|\nu=0; s=0; +\rangle$ can be assumed dominant, since its corresponding energy eigenvalue m^{*2} will be the lowest, and it appears in the exponent as seen from (2.12).

The rate in which the pions are created with a given p_T is proportional to the probability to find such a pion:

$$\frac{dN_\pi(p_T)}{dt dz p_T dp_T} \propto \mathcal{P}_\pi(p_T). \quad (4.7)$$

This probability, denoted here as $\mathcal{P}_\pi(p_T)$, is given by the convolution of probabilities for producing a quark and an antiquark whose transverse momenta add to the p_T of that given pion. More explicitly

$$\begin{aligned} \mathcal{P}_\pi(\mathbf{p}_T) &\propto \int \int d\mathbf{p}_{T,1} d\mathbf{p}_{T,2} \mathcal{P}_q(\mathbf{p}_{T,1}) \mathcal{P}_{\bar{q}}(\mathbf{p}_{T,2}) \\ &\quad \times \delta(\mathbf{p}_T - \mathbf{p}_{T,1} - \mathbf{p}_{T,2}) G(|\mathbf{p}_{T,1} - \mathbf{p}_{T,2}|), \end{aligned} \quad (4.8)$$

where the coalescence function $G(|\mathbf{p}_{T,1} - \mathbf{p}_{T,2}|)$ specifies the probability for a quark and an antiquark with a transverse momentum difference $\mathbf{p}_{T,1} - \mathbf{p}_{T,2}$ to form a pion. In this paper we assume the binding of the quark and antiquark to form a pion arises from a longitudinal “yo-yo” motion [12], independent of the transverse direction. Therefore we take $G=1$. (Other forms of G can be introduced if desired.) The pion distribution can then be evaluated analytically by applying the Faltung (folding) theorem which states that if we define

$$P_q(\mathbf{r}) \equiv \frac{1}{2\pi} \int d\mathbf{p}_{T,1} e^{-i\mathbf{p}_{T,1}\cdot\mathbf{r}} \mathcal{P}(\mathbf{p}_{T,1}), \quad (4.9a)$$

$$P_{\bar{q}}(\mathbf{r}) \equiv \frac{1}{2\pi} \int d\mathbf{p}_{T,2} e^{-i\mathbf{p}_{T,2}\cdot\mathbf{r}} \mathcal{P}(\mathbf{p}_{T,2}), \quad (4.9b)$$

and

$$\mathcal{P}_\pi(\mathbf{p}_T) \equiv \frac{1}{2\pi} \int d\mathbf{r} e^{i\mathbf{p}_T\cdot\mathbf{r}} P_\pi(\mathbf{r}), \quad (4.9c)$$

then

$$P_\pi(\mathbf{r}) \propto 2\pi P_q(\mathbf{r}) P_{\bar{q}}(\mathbf{r}). \quad (4.10)$$

Let us denote the operation of taking the Fourier transform by $\hat{\mathcal{F}}$, for example, $\mathcal{P}(p_T) = \hat{\mathcal{F}}[P(r)]$, and inversely $P(r) = \hat{\mathcal{F}}^{-1}[\mathcal{P}(p_T)]$. From (3.7), it is clear that the two-dimensional Fourier transform of a function, $P(r)$, with angular dependence $\exp(i\nu\phi)$, is

$$\mathcal{P}(p_T) \equiv \hat{\mathcal{F}}[P(r)] = \int_0^\infty dr r J_\nu(p_T r) P(r). \quad (4.11a)$$

Consequently

$$P(p_T) \equiv \hat{\mathcal{F}}[\mathcal{P}(p_T)] = \int_0^\infty dp_T p_T J_\nu(p_T r) \mathcal{P}(p_T). \quad (4.11b)$$

In our notation $\mathcal{P}_\pi(p_T) = \hat{\mathcal{F}}[P_\pi(r)]$, and since the probability to create a quark is equal to that of creating an antiquark, Eq. (4.10) implies that $P_\pi(r) \propto |P_q(r)|^2$. We shall assume that, just as in the case for a square well, the probability to create a quark is dominated by one wave function. This is indicated in (4.6), which claims that approximately $P_q(p_T) \propto |\mathcal{R}(p_T)|^2$. Here, $\mathcal{R}(p_T)$ is the ground-state wave function in momentum space, for which $\nu=0$. Combining all these results, we find the pion p_T spectra $\mathcal{P}_\pi(p_T)$ from $R(r)$:

$$\mathcal{P}_\pi(p_T) \propto \hat{\mathcal{F}} \left\{ \left[\hat{\mathcal{F}}^{-1} \left[\left\{ \hat{\mathcal{F}}[R(r)] \right\}^2 \right] \right]^2 \right\}. \quad (4.12)$$

Or inversely, if one is given the measured p_T distributions, $\mathcal{P}_\pi(p_T)$, one can find the ground-state wave function $R(r)$ by applying the following set of operations:

$$R(r) \propto \hat{\mathcal{F}}^{-1} \left\{ \hat{\mathcal{F}} \left[\hat{\mathcal{F}}^{-1} [\mathcal{P}_\pi(p_T)] \right]^{1/2} \right\}^{1/2}. \quad (4.13)$$

Equations (4.12) and (4.13) constitute some of the main results of the present investigation. They provide a direct transcription from the p_T spectra to the transverse ground-state wave function of the quark, and vice versa.

If we take the data of Alper *et al.* [5] for $p+p \rightarrow \pi^+ X$ at $\sqrt{s}=30.6$ GeV and $\theta_{c.m.}=89^\circ$, the p_T distribution can be fit very well with the parametrization

$$\begin{aligned} \mathcal{P}_\pi(p_T) &\propto \frac{1}{(m_T)^\lambda} \exp \left[-\frac{m_T}{T_a} \right], \\ m_T &\equiv \sqrt{p_T^2 + m_\pi^2}, \end{aligned} \quad (4.14)$$

where $m_\pi=140$ MeV is the mass of the pion. The best parametrization turned out to be $T_a=290$ MeV and $\lambda=1.5$. This fit of the data [5] is presented in Fig. 3. Note that T_a is not the usual “temperature,” since out fit is different from the usual $\exp(-p_T/T)$. From this parametrization of $\mathcal{P}_\pi(p_T)$, one can calculate the wave function $R(r)$ by carrying out the series of operations described by (4.13). Although it is not easy to form an exact analytical evaluation of $R(r)$, it can be carried out approximately, as shown in Appendix B. By taking the modified Bessel function $K_\mu(z)$ as $\approx \sqrt{\pi/2z} e^{-z}$, the wave function turns out to be roughly (see Appendix B)

$$R(r) \cong \left[\frac{5-2\lambda}{\pi} \right]^{1/2} T_a [1 + (2T_a r)^2]^{\lambda/4 - 9/8} \quad \text{for } \lambda < 5/2, \quad (4.15)$$

and, for $\lambda=1.5$,

$$R(r) \cong \sqrt{2/\pi} T_a [1 + (2T_a r)^2]^{-3/4}, \quad (4.16)$$

which shows that the wave function goes like $r^{-3/2}$ for $r \rightarrow \infty$, a rather slow decay for large distances.

The approximation we used for the modified Bessel function is good only for large z . Since the Fourier transform involves the whole region of z , the result (4.15) pro-

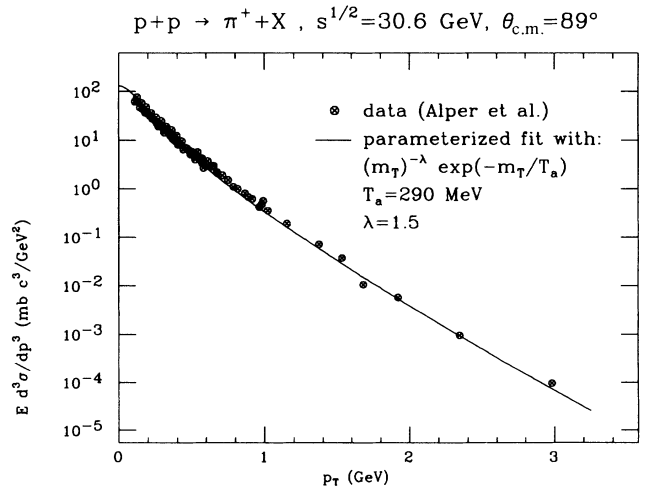


FIG. 3. p - p data from Alper *et al.*, fit here with $m_T^{-\lambda} \exp(-m_T/T_a) \times \text{const}$, having $T_a=290$ MeV and $\lambda=1.5$.

vides only a guide for the type of functions one expects after the series of operation (4.13). Changing direction, it is possible to start with $R(r)$ and to obtain $\mathcal{P}_\pi(p_T)$, by carrying out the operations in Eq. (4.12). We can use $R(r)$ as in (4.15), leaving the parameters T_a and λ free to fit the data. In other words, we replaced the approximate sign in (4.16) with an equality and chose

$$R(r) = \sqrt{2/\pi} T_b [1 + (2T_b r)^2]^{\lambda/4 - 9/8}. \quad (4.17)$$

Doing this, we found that $\lambda = 1.5$ agreed well with the calculation, but T_a in (4.16) could do with an adjustment, and was replaced with the value $T_b = 200$ MeV in (4.2) to be the best fit of the data [5] (see Fig. 4). The difference between T_a and T_b gives an estimate of the error in (4.15) and (4.16). The wave function (4.17), which leads to the fit in Fig. 4, is given in Fig. 5.

Given the wave function, one can find out the potential that would produce it. One may apply Eq. (4.1a), neglecting $m'(r)$ and taking $\nu = 0$:

$$m^2(r) = m^{*2} + R^{-1}(r) \frac{1}{r} \frac{\partial}{\partial r} r \frac{\partial}{\partial r} R(r). \quad (4.18)$$

This gives

$$m^2(r) = m^{*2} + 4 \left[\frac{9}{8} - \frac{\lambda}{4} \right] \frac{(9/8 - \lambda/4)r^2 - (2T_b)^{-2}}{[r^2 + (2T_b)^{-2}]^2}, \quad (4.19)$$

and for $\lambda = 1.5$

$$m^2(r) = m^{*2} + \frac{3}{4} \frac{3r^2 - T_b^{-2}}{[r^2 + (2T_b)^{-2}]^2} \quad (4.20)$$

which is the radial scalar potential for the flux tube. The potential (4.20) is given in Fig. 6.

The classical turning point r_c can be interpreted as the radius of the flux tube, just as r_0 in Fig. 1 is the classical

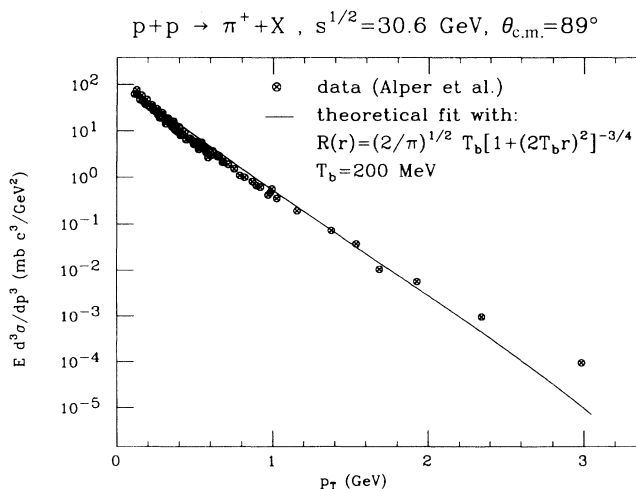


FIG. 4. The p - p data points from Alper *et al.*, and a solid curve corresponding to the p_T spectra calculated with the wave function $R(r)$ given by Eq. (4.17).

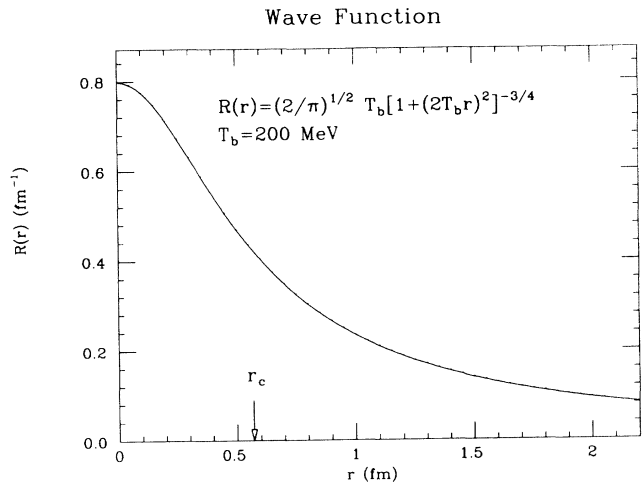


FIG. 5. The wave function $R(r)$ given by (4.17) with $T_b = 200$ MeV and $\lambda = 1.5$ which produced the solid curve in Fig. 4. The classical turning point r_c around 0.57 fm is indicated by the arrow.

turning point for a sharp boundary. It is given by setting $V(r_c) - E = 0$ in the Schrödinger equation. Since $V - E$ here corresponds to $m^2(r) - m^{*2}$ [see Eq. (4.1)], the relation (4.20) will give

$$r_c = \frac{1}{\sqrt{9/2 - \lambda T_b}} = \frac{1}{\sqrt{3} T_b} = 0.57 \text{ fm}. \quad (4.21)$$

This value is reasonable for a $q\bar{q}$ string. For a general fit of the form (4.14), the size of the string will be derived from (4.19). In other words, a given experimental p_T distribution will imply an approximate size of the tube by the prescription

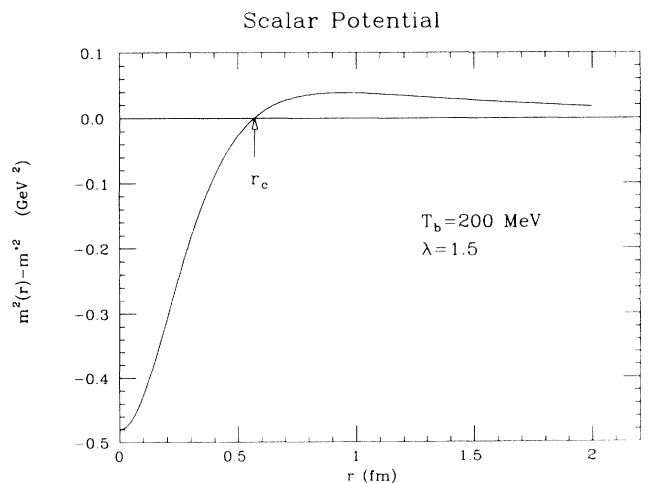


FIG. 6. The potential given by (4.20) with $T_b = 200$ MeV and $\lambda = 1.5$. It can always be shifted by a constant, as only $V - E$ affects the wave function in the Schrödinger equation. The classical turning point r_c around 0.57 fm is indicated by the arrow.

$$\mathcal{P}_\pi(p_T) \propto \frac{1}{(m_T)^\lambda} \exp\left[-\frac{m_T}{T_a}\right] \Rightarrow r_c \cong \frac{1}{\sqrt{9/2 - \lambda T_a}}, \quad (4.22)$$

correct up to $\sim 30\%$.

V. SUMMARY AND CONCLUSIONS

Recognizing that the p_T spectra of soft-produced mesons contain information on the motion of the quarks and antiquarks which form these mesons, we extract this information in the context of the flux-tube model with Schwinger's mechanism for particle production. This is carried out by assuming that an observed pion comes from combining a produced quark and a produced antiquark. Therefore, the transverse momentum distribution of the observed pions comes from the convolution of the transverse momenta distributions for the produced quarks and the produced antiquarks.

We introduce a smoothly varying scalar potential and consider the motion of a quark (or an antiquark) in a strong external field. We calculate the production rate of the quarks and pions as a function of p_T . We show how the experimental p_T spectra of pions produced in p - p collisions can be used to determine the transverse wave function of the quark and vice versa, using Fourier transforms. Based on some simplifying assumptions, the results are Eqs. (4.12) and (4.13). Knowing the transverse wave functions we can obtain the effective potential that would generate it.

From such a program, we find that the shape of the effective potential in the interior region is what one would expect. That is, the potential rises from the center of the flux tube, and the classical turning point is of the order of 0.6 fm, implying a classical size of the tube of this magnitude. This size is close to the common estimate [3] of ~ 0.5 fm. Nevertheless, the effective potential flattens out considerably beyond that point. For large r the potential goes like $\sim 1/r^2$. Consequently, the wave function decays slowly in the transverse direction as $r^{-3/2}$ for larger r , and extends much beyond the classical turning point. The root-mean-square radius of the quark wave function is 1.9 fm, which is considerably larger than the classical turning point. Such a slow decay is a surprising result. There appears to be a considerable motion of the quarks in the transverse direction. In this regard, it is of interest to note that the size of the tube one obtains in a lattice gauge calculation is quite thick [13], of the order of one-half the longitudinal length of the tube for a system in equilibrium. The evidence presented here may be the first indication of the extensive transverse motion of the quarks, and is qualitatively con-

sistent with the lattice calculations in a different context.

In conclusion, our result indicates that the p_T distribution of soft mesons originates from an effective potential the quark experience in the transverse direction that allows a substantial excursion of the quark into the classically forbidden region. That region is beyond 0.6 fm, which is the classical size of our tube. The tube flux model, which was developed initially for p - p collision, has since been applied to A - A collision at energies reached at the BNL Relativistic Heavy Ion Collider (RHIC) [14]. The p_T distribution for A - A collisions is very similar to p - p , and even with almost identical parameters [6]. Nucleus-nucleus collisions at zero-impact parameter have at least two radial length scales: the radius of the elementary $q\bar{q}$ string (calculated here ~ 0.6 fm) and the radius of the colliding nuclei $\sim 1.2 A^{1/3}$ fm. Nevertheless, these processes occur at a "real" temperature of $T \approx 200$ MeV, which adds another length scale ($1/T \approx 1$ fm). A detailed calculation of the p_T profile for A - A collisions is necessary. It will help us to distinguish between the $q\bar{q}$ string effects and thermal effects, and could lead us to the conquest of the desired holy grail, i.e., the quark-gluon plasma.

ACKNOWLEDGMENTS

The authors wish to thank T. Awes, C. Bottcher, and D. J. Dean for several comments. This research was sponsored by the U.S. Department of Energy under Contract No. DE-AC05-84OR21400, managed by Martin Marietta Energy Systems, Inc.

APPENDIX A: RECOVERING THE SCHWINGER LIMIT WHEN $r_0 \rightarrow \infty$

The Schwinger limit is Eq. (2.13) with m^{*2} replaced by $p_T^2 + m^2$. That limit can be derived from (3.15) setting $r_0 \rightarrow \infty$, as one should expect. In that case, one can use the asymptotic form for the Bessel function, i.e.,

$$\lim_{x \rightarrow \infty} J_\nu(x) \cong \left[\frac{2}{\pi x} \right]^{1/2} \cos \left[x - \frac{\nu\pi}{2} - \frac{\pi}{4} \right], \quad (A1)$$

and the expression in curly brackets in (3.15a) becomes simply $\mathcal{J}_{\mu,s,\pm}(\infty)$. After setting $r_0 \rightarrow \infty$ in the integral (3.8), one obtains

$$\mathcal{J}_{\nu,s,\pm}(\infty) = \frac{1}{p_T} \delta(p_T - C_{\nu,s,\pm}). \quad (A2)$$

Substituting this result in (3.15), one notices that $\delta^2(p_T - C_{\nu,s,\pm}) = \delta(p_T - C_{\nu,s,\pm})\delta(0)$, and $\delta(0)$ is just a volume element which disappears in the normalization in the denominator of (3.15). Hence this will give use the result

$$\lim_{r_0 \rightarrow \infty} \frac{dN_q}{dt dz p_T dp_T} = -2N_c \frac{\kappa}{4\pi^2} \sum_{\nu,s,\pm} \ln \left[1 - \exp - \frac{\pi(C_{\nu,s,\pm}^2 + m^2)}{\kappa} \right] \frac{\delta(p_T - C_{\nu,s,\pm})}{2\pi C_{\nu,s,\pm}}. \quad (A3)$$

All that is left now is to replace the discrete sum over all the coefficients found by Pavel and Brink [8] by a continuous integral. This is easily done if one recognizes that the quantum number ν is associated with an azimuthal angle as in (2.16), and that the quantum number s counts the allowed frequencies necessary to form standing waves which satisfy

the boundary condition. Therefore summing over ν, s, \pm becomes an integral over all allowed momenta. When $r_0 \rightarrow \infty$ the solutions are sufficiently dense to become an integral. At the limit where every point in momentum space is a solution, then $\sum_{\nu, s, \pm} \rightarrow \Delta x \Delta y \times 2\pi \int C dC$, and consequently one recovers Schwinger's result [1]

$$\lim_{r_0 \rightarrow \infty} \frac{dN_q}{d^4x} = -2N_c \frac{\kappa}{4\pi^2} \int dp_T p_T \ln \left[1 - \exp - \frac{\pi(p_T^2 + m^2)}{\kappa} \right]. \quad (\text{A4})$$

APPENDIX B: DERIVING THE WAVE FUNCTION FROM THE p_T DISTRIBUTION

We shall evaluate the wave function $R(r)$ in (4.15) from the experimental data [5] parametrized by (4.14), using the relation (4.13). The multiple operation (4.13) is usually not possible analytically; however, in some cases it can be carried out approximately. For the type of functions as in (4.14) it is useful to know the Hankel-Nicholson-type integrals [15]:

$$\int_0^\infty dr \frac{r^{\nu+1} J_\nu(ar)}{(r^2+z^2)^{\mu+1}} = \frac{a^\mu z^{\nu-\mu}}{2^\mu \Gamma(\mu+1)} K_{\nu-\mu}(az) \quad (a > 0, \text{Re} z > 0, -1 < \text{Re} \nu < 2\text{Re} \mu + 3/2). \quad (\text{B1})$$

For our purposes, using our notation

$$\hat{\mathcal{F}} \left[\frac{1}{(r^2 + T_a^{-2})^{\mu+1}} \right] \propto p_T^\mu K_{-\mu}(p_T/T_a), \quad \hat{\mathcal{F}}^{-1}[p_T^\mu K_{-\mu}(p_T/T_a)] \propto \frac{1}{(r^2 + T_a^{-2})^{\mu+1}}. \quad (\text{B2})$$

For large enough z , the modified Bessel functions are approximately

$$K_\mu(z) \approx \sqrt{\pi/2z} e^{-z} \quad (\text{B3})$$

for all μ . We neglect the mass of the pion, $m_T \approx p_T$, and approximate $\sigma(p_T)$ as $p_T^{1/2-\lambda} K_{\lambda-1/2}(p_T/T_a)$. The order of μ at this level of approximation can always be chosen so that one can make use of Eq. (B2). Applying formula (4.13), we get

$$R(r) \approx \hat{\mathcal{F}}^{-1} \sqrt{p_T^{(1/4-\lambda/2)} K_{1/4+\lambda/2}(p_T/T_a)}. \quad (\text{B4})$$

This can be approximated again by using the exponential approximation for the modified Bessel functions, which will imply that

$$\sqrt{K_\mu(z)} \approx (z/2\pi)^{1/4} K_{\mu'}(z/2) \quad (\text{B5})$$

for any μ and μ' . Applying (B2) again will produce Eq. (4.15).

-
- [1] J. Schwinger, Phys. Rev. **82**, 664 (1951).
[2] E. Brezin and C. Itzykson, Phys. Rev. D **2**, 1191 (1970).
[3] A. Casher, H. Neuberger, and S. Nussinov, Phys. Rev. D **20**, 179 (1979); H. Neuberger, *ibid.* **20**, 2936 (1979); C. B. Chiu and S. Nussinov, *ibid.* **20**, 945 (1979).
[4] R. C. Wang and C. Y. Wong, Phys. Rev. D **38**, 348 (1988), and references cited therein.
[5] B. Alper *et al.*, Phys. Lett. **47B**, 75 (1973); Nucl. Phys. **B87**, 19 (1975).
[6] For a review on transverse momentum distributions, see J. Schukraft, invited talk presented at the International Workshop on Quark-Gluon Plasma Signatures, Strasbourg, France, 1990, Report No. CERN-PPE/91-04 (unpublished).
[7] C. Martin and D. Vautherin, Phys. Rev. D **38**, 3593 (1988); **40**, 1667 (1989).
[8] H. P. Pavel and D. M. Brink, Z. Phys. C **51**, 119 (1991).
[9] Th. Schönfeld, A. Schäfer, B. Müller, K. Sailer, J. Reinhardt, and W. Greiner, Phys. Lett. B **247**, 5 (1990).
[10] K. Sailer, Th. Schönfeld, A. Schäfer, B. Müller, and W. Greiner, Phys. Lett. B **240**, 381 (1990).
[11] M. Herrmann and J. Knoll, Phys. Lett. B **234**, 437 (1990).
[12] X. Artru and G. Mennessier, Nucl. Phys. **B70**, 93 (1974); B. Andersson, G. Gustafson, and B. Söderberg, Z. Phys. C **20**, 317 (1983).
[13] S. L. Adler and T. Piran, Rev. Mod. Phys. **56**, 1 (1984); R. Sommer, Nucl. Phys. **B291**, 673 (1987).
[14] F. Low, Phys. Rev. D **12**, 163 (1975); S. Nussinov, Phys. Rev. Lett. **34**, 1286 (1975); N. K. Glendenning, and T. Matsui, Phys. Rev. D **28**, 2890 (1983); M. Gyulassy and A. Iwazaki, Phys. Lett. **165B**, 157 (1985); A. Kerman, T. Matsui, and B. Svetitsky, Phys. Rev. Lett. **56**, 219 (1986); G. Gatoff, A. K. Kerman, and T. Matsui, Phys. Rev. D **36**, 114 (1987); G. Gatoff, A. K. Kerman, and D. Vautherin, *ibid.* **38**, 96 (1988); A. Dyrek and W. Florkowski, Acta Phys. Pol. B **19**, 947 (1988); M. Kataja and T. Matsui, Ann. Phys. (N.Y.) **192**, 383 (1989).
[15] M. Abramowitz and I. Stegun, *Handbook of Mathematical Functions* (Dover, New York, 1972).